

Synthesis of Multi-Walled Carbon Nanotubes/ZnO Nanocomposites Using Absorbent Cotton

Jiao Qu^{1,2,*}, Chunqiu Luo^{1,*}, Qiao Cong¹

(Received 3 June 2011; accepted 6 July 2011; published online 18 July 2011).

Abstract: This letter focuses on the synthesis of multi-walled carbon nanotubes (MWNTs) and MWNTs/ZnO nanocomposites using absorbent cotton. The MWNTs have been synthesized by a rapid heating of absorbent cotton at different temperature (400°C, 550°C, 600°C). The MWNTs/ZnO nanocomposites have been synthesized by heating mixtures of Zn(OH)₂/H₂O/absorbent cotton at different temperature (at about 550°C and 600°C). The X-ray diffraction (XRD) pattern and energy dispersive spectrum (EDS) clearly show that the pure MWNTs and ZnO nanocomposites (with a mean size of 35.9 nm) were synthesized. The scanning electron microscopy (SEM) images demonstrate that the structure of synthesized MWNTs was middle-hollow, with inner and outer diameter of around 10 and 80 nm. The ZnO nanocomposites that had grown on the walls of MWNTs were nonuniform and agglomerated, with an outer diameter of around 110 nm. The selected area diffraction (SAD) patterns and Raman spectrum indicate that the MWNTs were well-crystallised, and there are a few defects in the walls. Infrared absorption spectroscopy (IR) spectra suggest that the surface of MWNTs has been covered by ZnO.

Keywords: MWNT; MWNTs/ZnO nanocomposites; Characteristic

Citation: Jiao Qu, Chunqiu Luo and Qiao Cong, "Synthesis of Multi-walled Carbon Nanotubes/ZnO Nanocomposites Using Absorbent Cotton", *Nano-Micro Lett.* 3 (2), 115-120 (2011). <http://dx.doi.org/10.3786/nml.v3i2.p115-120>

Introduction

In recent years, there has been an increasing interest in developing materials with low dimensional nanostructure such as nanotubes and nanocrystals due to their potential applications in nanoscale devices. Multi-walled carbon nanotubes (MWNTs) have attracted considerable attention owing to their chemical stability, unique electrical property, and extraordinary strength [1]. The commonest fabrication techniques are electric arc discharge [2,3], laser ablation [4,5], chemical vapor deposition (CVD) [6,7], and flame synthesis [8]. Although many efforts have been made in developing those methods above, high temperature, complicated control, and expensive or unrenewable materials are always needed.

Zinc Oxide (ZnO), with a wide direct bandgap (3.37 eV) at room temperature, is an important semiconductor material applied in conventional catalysis process. ZnO nanostructures have profound applications in optics, optoelectronics, and actuators due to many unique properties such as good optical activity, better sensitivity for UV light, high stability, catalytic activity, and low production cost [9-11]. In our previous work, ZnO nanoparticles have been successfully synthesized using plants [12,13]. Recently, ZnO nanocomposites grown onto MWNTs could reduce the threshold electric field because ZnO has smaller electron affinity than the MWNTs, and the MWNTs/ZnO nanocomposites junction is similar to a ZnO/metal junction allowing electrons to be easily emitted into a vacuum [14,15].

It is well known that cotton contains a large amount

¹School of Chemistry and Chemical Engineering, Bohai University, Jinzhou 121013, China

²School of Urban and Environmental Sciences, Northeast Normal University, Changchun 130024, China

*Corresponding author. E-mail: qujiao@bhu.edu.cn; fplj_lcq@163.com; Tel: +864163400302; Fax: +864163400161.

of vascular bundles, and their components are cellulose, hemicellulose, and lignin. The present work shows that MWNTs can be obtained by heating grass containing much tubular cellulose in the presence of a suitable amount of oxygen [16,17]. The treatments of removing protein and grease in the synthetic method of MWNTs from vascular bundles will be unnecessary if the absorbent cotton is used as the source of carbon. In this work, MWNTs and MWNTs/ZnO nanocomposites were synthesized using absorbent cotton as the source of carbon, and characterized using special technique explained under experimental section. To our knowledge, this is the first report on the synthesis of MWNTs and MWNTs/ZnO nanocomposites using absorbent cotton. The method of synthesizing MWNTs and MWNTs/ZnO nanocomposites using absorbent cotton may be adaptable to industry.

Materials and Methods

Materials

Absorbent cotton and ZnO powders were purchased from the market and used without any further purification.

Synthesis of MWNTs

0.9 g absorbent cotton was rolled out onto the crucible, put into the muffle furnace, heated to about 400°C rapidly, and kept at about 400°C for 3 min. Subsequently, the samples were cooled to room temperature. The heat treatment (at about 400°C) was repeated many times and the products containing MWNTs were collected. Finally, the collected products were washed 3 times with ethanol and water to remove impurities, and oven-dried at 105°C for 72 h.

Similarly, the above processes were treated at 550°C, 600°C, respectively.

Synthesis of MWNTs/ZnO Nanocomposites

Absorbent cotton was added into the solution of Zn(OH)₂ (3 g ZnO dissolved in 100 ml water), and shaken (300 rpm) at 25°C for 72 h. Afterward, the absorbent cotton with Zn(OH)₂ was dried in an oven at 105°C for 24 h, and treated with the above processes (as shown in 2.2 fraction) at 550°C and 600°C, respectively.

Characterization

The products were characterized by the methods as follows: X-ray diffraction (XRD) patterns were carried out with the Al K α line as the excitation source ($h\nu=1486.6\text{ eV}$) using a PHI 5000C (Perkin-Elmer, USA); scanning electron microscopy (SEM) images were performed using a JEOL JSM-840 operated at 20 kV; and energy dispersive spectra (EDS) were obtained using an Oxford EDX system attached to SEM. The products containing MWNTs were characterized further by the following methods: selected area diffraction (SAD) pattern was taken on high resolution scanning electron microscopy attached to SEM; Raman spectrum was obtained using a micro-Raman spectrometer (Nicolet Almega XR) with a 473 nm laser as an excitation source; Infrared absorption spectroscopy (IR) spectra (4000~400 cm⁻¹) were measured using a IR spectrometer (Nicolet Antaris II).

Results and Discussion

The XRD patterns of the powdered MWNTs and the MWNTs/ZnO nanocomposites synthesized in 600°C are shown in Fig. 1. From Fig. 1(a), the characteristic peak at $2\theta=25.8^\circ$ represents graphite peak corresponding to C of the MWNTs and reveals the crystallinity of the MWNTs [18]. Moreover, the peaks at other degrees are observed clearly in the profile. It indicates that some impurities were combined in the walls

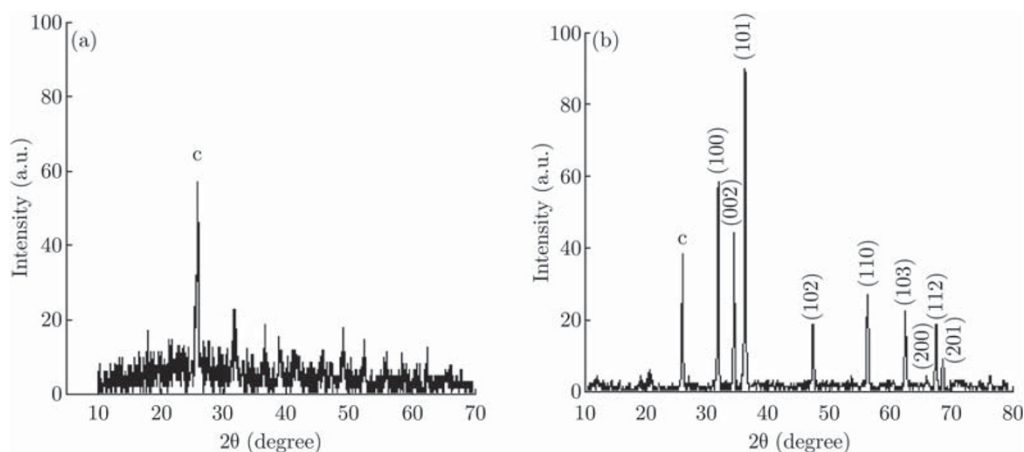
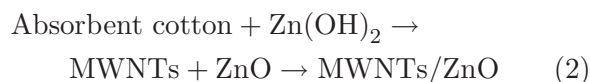
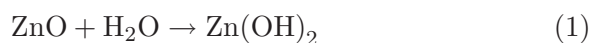


Fig. 1 XRD patterns of the products: (a) containing MWNTs, (b) containing MWNTs/ZnO nanocomposites.

of synthesized MWNTs. The diffractions of both MWNTs and ZnO could be observed in Fig. 1(b). Except the peak corresponding to C of the MWNTs, the XRD peaks reveal good agreements with ZnO (JCPDS 36-1451). The main dominant peaks for ZnO are identified at $2\theta=31.76^\circ$, 34.43° , 36.20° , 47.48° , 56.45° , 62.77° , 66.27° , 67.88° and 68.99° , which can be indexed as (100), (002), (101), (102), (110), (103), (200), (112), (201) planes of ZnO, respectively. The main diffraction peaks related to the impurities are not observed, it means that the MWNTs/ZnO nanocomposites were pure.

The ZnO nanocomposites grown onto the surface of MWNTs may be produced by the following process:



XRD results of ZnO show prominent 100, 002 and 101 reflections among which 101 is of high-

est intensity [19-21]. The diameter (D) of the ZnO nanoparticles was calculated using the Debye-Scherrer formula $D=K\lambda/(\beta\cos\theta)$, where K is the Scherrer constant (0.9 in this study), λ is the X-ray wave length, β is the peak width at half-maximum, and θ is the Bragg diffraction angle. The XRD peaks show that the ZnO nanoparticles had a diameter of about 35.9 nm. Furthermore, the dominant peaks of ZnO were more intensive and narrower, which are in good agreements with the characteristic of the previously synthesized ZnO nanoparticles [12,22,23] and mean that a good crystalline nature of the ZnO have grown on the surface of MWNTs.

Figure 2 (a) shows the typical SEM images of the MWNTs. The walls are composed of graphite sheets aligned to the tube axis. The structures of individual MWNTs are middle-hollow. The outer and inner diameter is 80 and 10 nm, and the length of nanotubes observed is longer than $1\mu\text{m}$. As shown in Fig. 2(b), ZnO nanoparticles have grown on the surface of the MWNTs. The outer diameter of MWNTs/ZnO nanocomposites is about 110 nm.

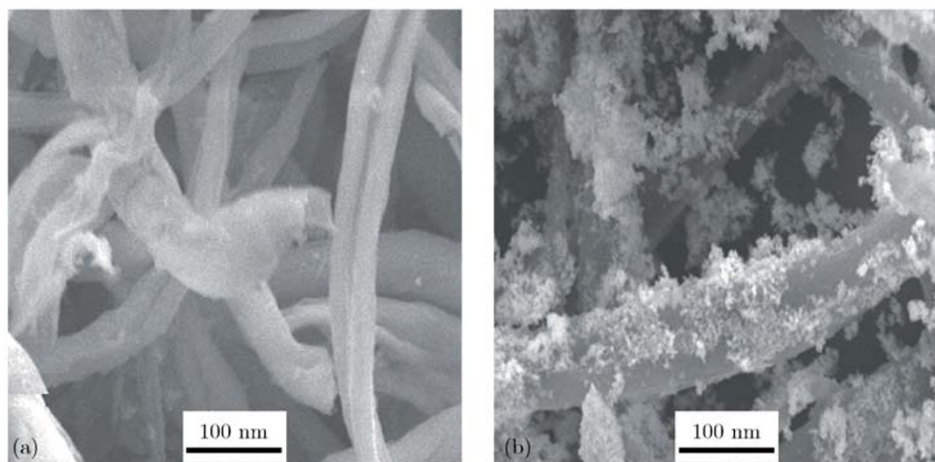


Fig. 2 SEM images of the products: (a) containing MWNTs, (b) containing MWNTs/ZnO nanocomposites.

To obtain the more details of the MWNTs, the structures of framework were characterized by SAD and Raman spectrum. The MWNTs are well-crystalline, which is resulted from SAD pattern in Fig. 3. The SAD pattern is characteristic of MWNTs, and the two elongated arcs and circle correspond to the planes of graphite carbon, which are consistent with the XRD results. The wall of the MWNTs is composed of high-quality graphite layers, but there are a few defects in the

walls of the MWNTs. It was proved further by the Raman spectrum (shown in Fig. 4). The peak at 1580 cm^{-1} (G-band) corresponds to an E_{2g} mode of graphite and is related to the vibration of sp²-bonded carbon atoms in a two-dimensional hexagonal lattice, such as in a graphite layer. Nanotubes with concentric multi-walled layers of the hexagonal carbon lattice display the same vibration. The D-band at around 1360 cm^{-1} is associated with vibrations of carbon atoms with dangling bonds in

plane terminations of disordered graphite or glassy carbons. The inverse of the ID/IG intensity ration between the G- and D- bands is a usual measure of the graphitic ordering and may also indicate the approximate layer size in the hexagonal plane, L_a [24,25]. In this work, the ID/IG ratio of the MWNTs is about 0.47. The length of nanotubes observed in SEM images is longer than $1\ \mu\text{m}$, which does not agree with the calculation using the formula $L_a=44(\text{ID}/\text{IG})-1$. This is consistent with the prior reports by Kang et al. [17].

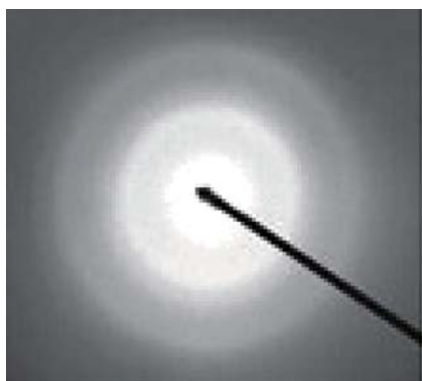


Fig. 3 SAD pattern of individual MWNTs.

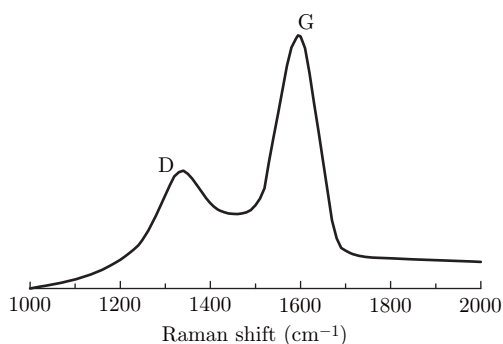


Fig. 4 Raman spectrum of the products containing MWNTs.

Here an important question emerged: are the tubelike carbon structures prepared with this method genuine multi-wall nanotubes or just a simple “open graphitic structures”. In botany, vascular bundles are a strand of conducting tissue extending lengthwise through the stems of plants, including ferns, fern allies, gymnosperms, and angiosperms. They have similar tubular structures, and the major compositions are also cellulose, hemicelluloses and lignin. In our experiment, four pieces of evidence are found which may support the result that the products are really

MWNTs. First, XRD pattern of the MWNTs indicates that the characteristic peak at $2\theta=25.8^\circ$ represents graphitic peak corresponding to C of the MWNTs and reveals the crystalline of the MWNTs. Second the high-resolution SEM image shows that the wall-to-wall distance is uniform, 80 nm, can be seen that the vascular bundles are still maintaining tubular structures, while it is nearly impossible for the open graphitic structures to obtain all such perfect structure. Third, the SAD pattern of the tube like carbon structures reveals that the products are single crystalline, which cannot form through a simple “open graphitic structures”. Fourth, the Raman spectrum exhibits no plane termination in the products combined with the straight figure. These evidences further confirm that the products are well-crystalline MWNTs.

During this approach, water is lost, first from that absorbed by the cellulose and then by β -elimination from the cellulose hydroxyls, which makes the tubular structures contract and realizes the formation of C=C double bonds. Simultaneously, the oxygen makes the pyrolytic reactions of the vascular bundles more rapid. The complex chemistry of the C-O-H system is also helpful in the synthesis of MWNTs. Base on these results and theories the formation of MWNTs is not the open graphitic structures.

As shown in Fig. 5, the influence of temperature on the synthesis of MWNTs and MWNTs/ZnO nanocomposites can be clarify briefly. The typical IR spectra of the samples which were obtained by heat treatments at about 400°C , 550°C and 600°C are shown in Fig. 5(a), (b), and (c). Figure 5(c) shows a typical IR spectrum of the finally obtained carbon nanotubes. The peak at $1569.5\ \text{cm}^{-1}$ is associated with the vibration of the carbon skeleton of the carbon nanotubes. The peaks at about 2368.7 and $2337.6\ \text{cm}^{-1}$ correspond to the C=C double bonds stretch vibration, originated from the surface of tubes [26]. The peaks at 1706.6 , $1130.2\ \text{cm}^{-1}$ indicate the existence of carboxylic groups on the tubes. The peak at $3867.3\ \text{cm}^{-1}$ corresponds to the stretching vibrations of OH groups. With the increasing of temperature, the peaks corresponding to carboxylic groups became more and more narrow and weak. These results mean that the

carboxylic groups were eliminated step by step, and the cellulose was converted into the carbon skeleton of the carbon nanotubes with the increasing of temperature. From Fig. 5(d) and (e), the IR spectra of MWNTs/ZnO nanocomposites are helpful to understand further the formation of them, which reveal the different surface chemistry of MWNTs and the MWNTs/ZnO nanocomposites. In the high frequency region, the weak peaks around $3516.0\sim 3948.0\text{ cm}^{-1}$ can be observed, which can be assigned to the stretching vibrations of OH groups. Compared with the IR spectra of MWNTs, the two peaks at 2368.7 and 2337.6 cm^{-1} became narrower, and the peaks around $1709.8\sim 1060.5\text{ cm}^{-1}$ are lower in the composite than those of MWNTs. The result suggests that the surface of MWNTs has been covered by ZnO. Furthermore, peaks observed at low frequency region (around $500\sim 700\text{ cm}^{-1}$) in MWNTs/ZnO nanocomposites are assigned to the Zn-O. Compared with Fig. 5(d), the peaks are weaker than them in the Fig. 5(e), and it is in agreement with the variation (see Fig. 5(b) and (c)). In addition, most of peaks can't be observed clearly which may be caused by noise.

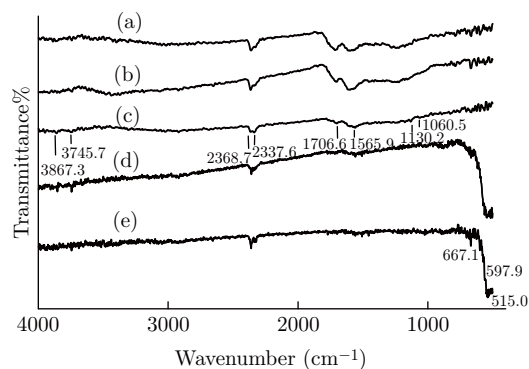


Fig. 5 IR spectra of the products: (a) containing MWNTs in 400°C , (b) containing MWNTs in 550°C , (c) containing MWNTs in 600°C obtained finally; (d) containing MWNTs/ZnO in 550°C , (e) containing MWNTs/ZnO in 600°C .

The result of Raman spectrum indicates there are some defects in the walls of MWNTs, which have potential applications in catalysis by using as catalyst supports [27]. Some ZnO particles were just covered on the surface of MWNTs via physical adsorption. At the same time, ZnO particles also can enter the defects in the walls of the MWNTs.

In the EDS spectrum of the MWNTs/ZnO nanocomposites, as shown in Fig. 6, the peaks

of C, O and Zn are obviously observed. The peak of Cu resulted from the conductive adhesive. It means that the MWNTs/ZnO nanocomposites were pure.

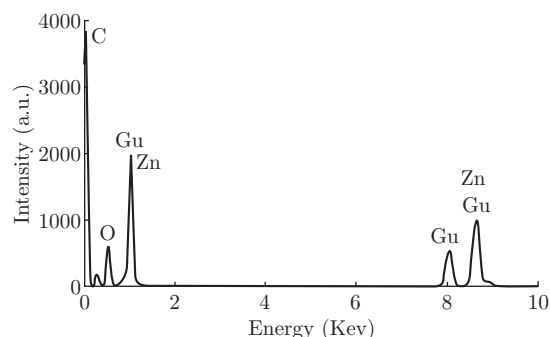


Fig. 6 EDS spectrum of the products containing MWNTs/ZnO nanocomposites.

Conclusion

In this work, MWNTs and MWNTs/ZnO nanocomposites were synthesized using absorbent cotton and ZnO powders. The MWNTs and MWNTs/ZnO nanocomposites were characterized by XRD, SEM, EDS, SAD, Raman spectrum, and IR. The results indicate that the pure MWNTs were synthesized. The structure of synthesized MWNTs was middle-hollow, with inner and outer diameter of around 10 and 80 nm. The ZnO nanocomposites that had grown on the walls of MWNTs were nonuniform and agglomerated, with an outer diameter of around 110 nm.

Acknowledgements

This work was partly supported by the National Natural Science Foundation of China (21003081), and the Liaoning Education Department Projects (2010010, 2006032).

References

- [1] S. Iijima, Nature 354, 56 (1991). <http://dx.doi.org/10.1038/354056a0>
- [2] H. W. Kroto, J. R. Heath, S. C. O'Brien, R. F. Curl and R. E. Smalley, Nature 318, 162 (1985). <http://dx.doi.org/10.1038/318162a0>
- [3] T. W. Ebbesen and P. M. Ajayan, Nature 358, 220 (1992). <http://dx.doi.org/10.1038/358220a0>
- [4] P. C. Eklund, B. K. Pradhan, U. J. Kim, Q. Xiong, J. E. Fischer, A. D. Friedman, B. C. Holloway, K. Jordan

- and M. W. Smith, *Nano Lett.* 2, 561 (2002). <http://dx.doi.org/10.1021/nl025515y>
- [5] W. K. Maser, E. Munoz, A. M. Benito, M. T. Martinez, G. F. Fuente, Y. Maniette, E. Anglaret and J. L. Sauvajol, *Chem. Phys. Lett.* 292, 587 (1998). [http://dx.doi.org/10.1016/S0009-2614\(98\)00776-3](http://dx.doi.org/10.1016/S0009-2614(98)00776-3)
- [6] D. S. Bethune, C. H. Kiang, M. S. Devries, G. Gorman, R. Savoy and R. Beyers, *Nature* 363, 605 (1993). <http://dx.doi.org/10.1038/363605a0>
- [7] Z. F. Ren, Z. P. Huang, J. W. Xu, J. H. Wang, P. Bush, M. P. Siegal and P. N. Provencio, *Science* 282, 1105 (1998). <http://dx.doi.org/10.1126/science.282.5391.1105>
- [8] R. L. Vanderwal, G. M. Berger and L. J. Hall, *J. Phys. Chem.* 106, 3564 (2002). <http://dx.doi.org/10.1021/jp012844q>
- [9] K. R. Lee, S. Park and J. H. Lee, *J. Mater. Sci. Lett.* 22, 65 (2003). <http://dx.doi.org/10.1023/A:1021738526590>
- [10] M. A. Gondal, Q. A. Drmosh, Z. H. Yamani and M. Rashid, *Int. J. Nanoparticles* 2, 142 (2009).
- [11] M. A. Gondal, Q. A. Drmosh, Z. H. Yamani and T. A. Saleh, *Appl. Surf. Sci.* 256, 298 (2009). <http://dx.doi.org/10.1016/j.apsusc.2009.08.019>
- [12] J. Qu, C. Q. Luo and J. X. Hou, *Micro. Nano. Lett.* 6, 174 (2011). <http://dx.doi.org/10.1049/mnl.2011.0004>
- [13] J. Qu, X. Yuan, X. H. Wang and P. Shao, *Environ. Pollut.* 159, 1783 (2011). <http://dx.doi.org/10.1016/j.envpol.2011.04.016>
- [14] K. Yu, Y. S. Zhang, F. Xu, Q. Li, Z. Q. Zhu and Q. Wan, *Appl. Phys. Lett.* 88, 153123 (2006). <http://dx.doi.org/10.1063/1.2195115>
- [15] J. Y. Pan, C. C. Zhu and Y. L. Gao, *Appl. Surf. Sci.* 254, 3787 (2008). <http://dx.doi.org/10.1016/j.apsusc.2007.12.002>
- [16] W. S. Cho, E. Shamada, Y. Kondo and K. Takayanagi, *Appl. Phys. Lett.* 69, 278 (1996). <http://dx.doi.org/10.1063/1.117949>
- [17] Z. H. Kang, E. B. Wang, B. D. Mao, Z. M. Su, L. Chen and L. Xu, *Nanotechnology* 16, 1192 (2005). <http://dx.doi.org/10.1088/0957-4484/16/8/036>
- [18] I. Sameera, R. Bhatia and V. Prasad, *Phys B: Condens. Matter*, 405, 1709 (2010). <http://dx.doi.org/10.1016/j.physb.2009.12.074>
- [19] Q. Zhou, R. M. Fleming, D. W. Murphy, C. H. Chen, R. C. Haddon, A. P. Ramirez and S. H. Glarum, *Science* 263, 1744 (1994). <http://dx.doi.org/10.1126/science.263.5154.1744>
- [20] F. Xu, P. Zhang, A. Navrotsky, Z. Yuan, T. Ren, M. Halasa and B. Su, *Chem. Mater.* 19, 5680 (2007). <http://dx.doi.org/10.1021/cm071190g>
- [21] H. F. McMurdie, M. C. Morris, E. H. Evans, B. Paretzkin, W. Wong-Ng, L. Ettlinger and C. R. Hubbard, *Powder Diffr.* 1, 64 (1986).
- [22] C. C. Chen, P. Liu and C. H. Lu, *J. Chem. Eng.* 144, 509 (2008). <http://dx.doi.org/10.1016/j.cej.2008.07.047>
- [23] C. He, T. Sasaki, Y. Shimizu and N. Koshizaki, *Appl. Surf. Sci.* 254, 2196 (2008). <http://dx.doi.org/10.1016/j.apsusc.2007.09.007>
- [24] J. M. Calderon-Moreno and M. Yoshimura, *J. Am. Chem. Soc.* 123, 741 (2001). <http://dx.doi.org/10.1021/ja003008h>
- [25] A. Kasuya, Y. Sasaki, Y. Saito, K. Tohji and Y. Nishina, *Phys. Rev. Lett.* 78, 4434 (1997). <http://dx.doi.org/10.1103/PhysRevLett.78.4434>
- [26] A. Yuan and Q. Zhang, *Electrochem. Commun.* 8, 1173 (2006). <http://dx.doi.org/10.1016/j.elecom.2006.05.018>
- [27] P. Serp, M. Corrias and P. Kalck, *Appl. Catal. A* 253, 337 (2003). [http://dx.doi.org/10.1016/S0926-860X\(03\)00549-0](http://dx.doi.org/10.1016/S0926-860X(03)00549-0)